Journal of
Materials Chemistry C

PAPER

Cite this: *J. Mater. Chem. C*, 2015, **3**, 1126

Intramolecular charge transfer (ICT) of a chiroptically active conjugated polymer showing green colour

Hirotsugu Kawashima, Kohsuke Kawabata and Hiromasa Goto*

A donor–acceptor type achiral monomer 4,7-bis(2,3-dihydrothieno[3,4-*b*]-1,4-dioxin-5-yl)-2,1,3-benzothiadiazole was synthesised and electrochemically polymerised in a cholesteric liquid crystalline (CLC) medium. This film exhibits a fingerprint pattern under the polarised optical microscopic observation. A possible mechanism of the fingerprint structure formation through a procedure of electrochemical polymerisation in a CLC medium is presented. The preparation of chiral polymer films even from achiral monomers is demonstrated. The film shows green colour in the reduced state and blue in the oxidised state. Changes in colour and CD signals of the film are repeatable with electrochemical oxidation and reduction. The presence of radical cations in the chiral environment, referred to as chiralions, distributed along chiral polymer chains is proposed.

Received 21st September 2014
Accepted 1st December 2014

DOI: 10.1039/c4tc02124j

www.rsc.org/MaterialsC

1 Introduction

Conjugated polymers have attracted much attention because of their characteristic optical, electrochemical and magnetic properties.[1–4] Applications of these materials in photovoltaic cells,[5,6] light-emitting diodes,[7] organic field-effect transistors,[8] and opto-electronic devices[9–11] have motivated the development of synthesis and processing methods for conjugated polymeric materials. Electronic characters of these materials are primarily governed by the nature of the molecular conjugation. In addition, intramolecular and intermolecular interactions have considerable influence on the properties.[12,13] Higher-order structures of organic materials are dependent on these interactions and molecular shapes. A precise molecular design can lead to desirable, highly ordered structures for various applications. Therefore, micro- or mesostructural control of the materials is one of the key issues for obtaining the desired performance.

Liquid crystals (LCs) are considered mesophases between solid and liquid states. LCs have both fluidity and crystallinity; LC molecules can flow like a liquid, but are oriented like solid crystals at the mesoscopic level.[14–16] The cholesteric liquid crystalline (CLC) state is one of the chiral liquid crystalline states with a helical structure. This CLC state exhibits a twist between the individual molecules perpendicular to the director (a vector of molecular orientation). Assimilation of the asymmetric packing of CLC molecules affords formation of a longer-range helical chiral structure.[17,18] It is known that some insects such as golden beetles and jewel beetles have this kind of periodic, anisotropic structure on their body surface.[19] Hariyama *et al.* implied that the photonic insects use such structures for recognition of their sex.[20] Thus, the mesoscopic structures of CLC are involved in biological activity and in some biomimetic technologies.[21]

Electrochemical polymerisation is one of the methods to produce conjugated polymer films deposited directly on the electrodes.[22–24] Monomers in electrolytic solution are oxidised with application of potential. Then, radicals are generated on active sites of the monomers at the molecular level. Subsequently, radical polymerisation of the monomers proceeds on the electrode. Polymer films are thus deposited on the electrodes during polymerisation. Polymer films prepared by electrochemical polymerisation can be purified easily by washing with water and an organic solvent. The resultant films can be used for electro-optical devices such as electrolytic capacitors and display devices.[25–27]

The geometric structure of polymer films prepared by electrochemical polymerisation depends strongly on the conditions of the electrolytic solution and electrode surfaces.[28,29] Precise control of the conditions leads to favourable structures – regular and highly ordered.[30,31] Employment of CLC as a solvent of electrochemical polymerisation, in place of isotropic liquid solvents such as acetonitrile, allows us to transcribe the fingerprint texture of a CLC medium to a resulting film.[32–34] Textures of the film surfaces reflect CLC properties both structurally and optically, except that the textures are no longer flowing. Therefore, electrochemical polymerisation in a liquid crystalline medium can control meso- or macroscopic structures of the resultant polymer films.[35]

One of the important advantages of this method is to generate chiroptically active polymer films even from achiral

---

Division of Materials Science, Faculty of Pure and Applied Sciences, University of Tsukuba, Tsukuba, Ibaraki 305-8573, Japan. E-mail: gotoh@ims.tsukuba.ac.jp

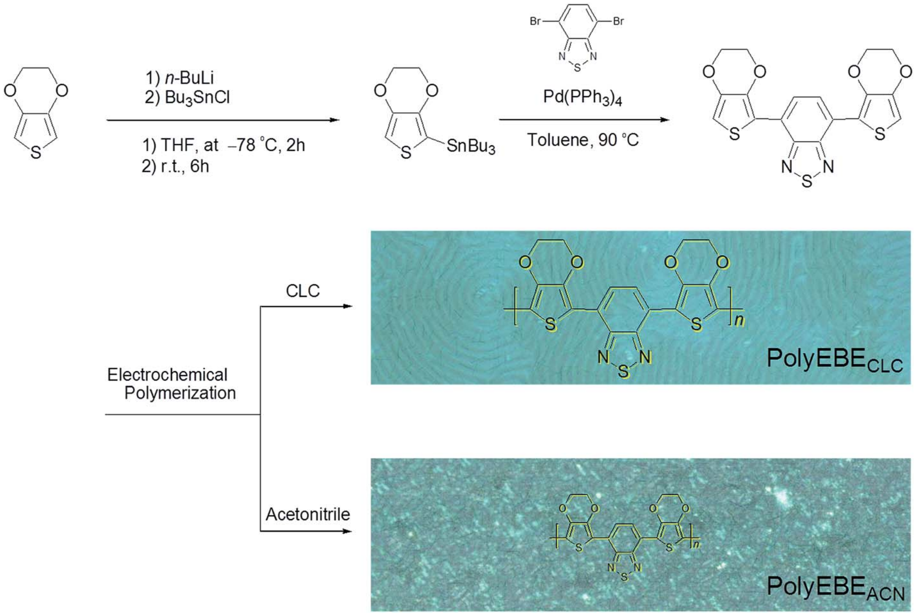

Scheme 1 Synthetic routes to polyEBE$_{CLC}$ and polyEBE$_{ACN}$.

monomers. In this research, we prepared an achiral monomer 4,7-bis(2,3-dihydrothieno[3,4-*b*]-1,4-dioxin-5-yl)-2,1,3-benzothiadiazole (EBE), consisting of an electron-donor–acceptor chemical structure, as shown in Scheme 1. Benzothiadiazole, as an electron acceptor, is sandwiched between two 2,3-dihydrothieno[3,4-*b*][1,4]dioxine (EDOTs), serving as electron donors. The low oxidation potential of EDOT units allows polymerisation under appropriate conditions.[36] Rod-like structures like EBE can show good affinity towards LCs, because LCs consist of rod-like molecules.[37] Therefore, EBE can be a suitable monomer for electrochemical polymerisation in a CLC medium.

Levent *et al.* previously demonstrated that a polymer resulting from EBE by electrochemical polymerisation exhibited green colour in the reduced state.[38,39] Green colour polymers are required for green pixels of full-colour electrochromic displays. The production of a green polymer requires an appropriate molecular design.[40–44] The absorption band of green polymers is in the blue and red ranges, with green light reflected. Our motivation in this study is to create low-bandgap, highly sensitive, and optically active polymer films for the realisation of full-colour chiral electrochromic displays.

2 Experimental section

Materials and methods

Chemicals were purchased from Tokyo Kasei Japan (TCI) and Merck. The reagents were used as received. ITO-coated glass (9 Ω cm^{-2}) was purchased from Furuuchi Chemical Corporation. ^{1}H NMR spectroscopy measurements were performed in $CDCl_3$ with an ECS 400 spectrometer (JEOL). Chemical shifts are reported in ppm downfield from $SiMe_4$ as an internal reference. Optical texture observations were carried out using an ECLIPS LV 100 high-resolution polarizing microscope (Nikon) with a LU Plan Fluor lens and a CFIUW lens (Nikon). Digital pictures were recorded by using an Optio RZ10 (Pentax). FTIR absorption spectra were obtained with an FT/IR-300 spectrometer (Jasco) using a KBr method. UV-vis absorption spectra were recorded on a V-630 UV-vis optical absorption spectrometer (Jasco). Electrochemical measurements were performed using an electrochemical analyzer, PGSTAT 12 (AUTOLAB). CD spectra were obtained with a J-720 spectrometer (Jasco).

Synthesis of tributyl(2,3-dihydrothieno[3,4-*b*][1,4]dioxin-5-yl) stannane

This compound was prepared by a previously reported method.[45] Quantities used: 2,3-dihydrothieno[3,4-*b*][1,4]dioxine (10.2 g, 71.4 mmol), tributylstannyl chloride (19.0 mL, 70.0 mmol), *n*-butyllithium (26.0 mL, 70.2 mmol), tetrahydrofuran (80 mL), and a colourless oil (4.93 g, 11.4 mmol, 16.3%). ^{1}H NMR (400 MHz, δ from TMS (ppm), $CDCl_3$): δ 0.89 (t, 9H, $-Sn-(CH_2)_3-CH_3$, $J = 7.2$ Hz), 1.09 (m, 6H, $-Sn-(CH_2)_2-CH_2-CH_3$), 1.32 (m, 6H, $-Sn-CH_2-CH_2-CH_2-CH_3$), 1.55 (t, 6H, $-Sn-CH_2-C_3H_7$, $J = 8.0$ Hz), 4.16 (s, 4H, $-O-CH_2-CH_2-O-$), 6.57 (s, 1H, 2*H* (thiophene)).

Synthesis of 4,7-bis(2,3-dihydrothieno[3,4-*b*]-1,4-dioxin-5-yl)-2,1,3-benzothiadiazole (EBE)

A solution of tributyl(2,3-dihydrothieno[3,4-*b*][1,4]dioxin-5-yl) stannane (285.6 mg, 0.66 mmol) and 4,7-dibromo-2,1,3-benzothiadiazole (101.9 mg, 0.37 mmol) in toluene (2 mL) was stirred for 30 min at 50 °C. Then, tetrakis(triphenylphosphine)palladium(0) (19.9 mg, 0.017 mmol) was added to the solution and refluxed for 1 day at 90 °C. After cooling, the mixture was washed with water, extracted with dichloromethane, and dried over $MgSO_4$. After filtration, the solvent was removed *in vacuo* and the crude material was purified by column chromatography (silica gel, ethyl acetate : *n*-hexane = 2 : 1). The product was dried *in vacuo* and isolated as a deep red solid (65.4 mg, 47.4%) ^{1}H NMR (400 MHz, δ from TMS (ppm), $CDCl_3$): δ 4.33 (m, 4H, –O–CH_2–CH_2–O– (outer)), 4.40 (m, 4H, –O–CH_2–CH_2–O– (inner)), 6.57 (s, 2H, 2*H* (thiophene)), 8.39 (s, 2H, 5,6*H* (benzene)).

3 Results and discussion

Constituents of the LC electrolytic solution for the reaction mixture for electrochemical polymerisation of EBE in a CLC are summarised in Table 1 (EBE, 0.89 wt%; 4-cyano-4′-*n*-hexylbyphenyl (6CB), 89.3 wt%; cholesterol oleyl carbonate (COC), 8.93 wt%; tetrabutylammonium perchlorate (TBAP), 0.89 wt% as a supporting electrolyte salt). 6CB, which exhibits liquid crystallinity at room temperature, is employed as an achiral liquid crystalline molecule. The addition of a small amount of a chiral compound as a chiral inducer to a nematic liquid crystal induces a cholesteric liquid crystal phase with structural chirality from an achiral nematic phase.[46]

The polymerisation process is summarised in Fig. 1. This reaction mixture was charged between transparent indium-tin-oxide (ITO) coated glasses, as an anode and a cathode (Fig. 1a). Visual inspection of the cell indicates the formation of a LC phase at room temperature (Fig. 1b). Then, a DC potential of 4.0 volts was applied across the cell and the polymerisation reaction was initiated for 30 min. The colour change of the cell indicates progress of the polymerisation (Fig. 1c). The remaining reaction mixture on the electrode (anode side) after the polymerisation was removed by washing with *n*-hexane (Fig. 1d).

Polarised optical microscopy (POM) observation reveals that the polyEBE film shows fingerprint textures, indicating transcription of the CLC texture to the polymer film (Fig. 2). We propose a mechanism of transcription of the CLC fingerprint texture during electrochemical polymerisation in CLC medium, as illustrated in Fig. 3. In a reaction mixture, monomers align along the directors of the LC before polymerisation (Fig. 3b). Electrochemical polymerisation progresses on the anode surface. The polymer grows along the orientation with an imprinted 3D aggregation structure of CLC. In this polymerisation process, the main chain grows independently with phase separation against 6CB and COC (Fig. 3c). The polymer film appears on the anode side in the electrochemical

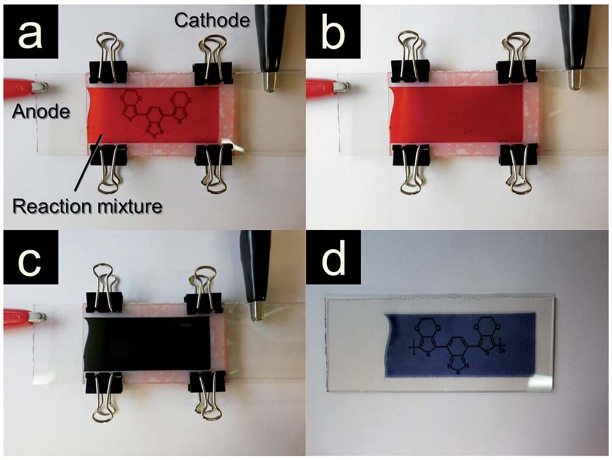

Fig. 1 Polymerisation procedure of EBE in CLC electrolytic medium. (a) Change of the reaction mixture (liquid phase) in a polymerisation cell. (b) Phase change of the mixture from liquid to cholesteric liquid crystal. (c) Colour change indicates successful progress of polymerisation. (d) Resulting polymer film after washing with *n*-hexane.

Table 1 Contents of the reaction mixture

Reagent	Chemical structure	wt%
4-Cyano-4′-*n*-hexylbiphenyl (6CB, liquid crystal)	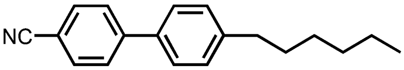	89.3
Cholesteric oleyl carbonate (chiral inducer)	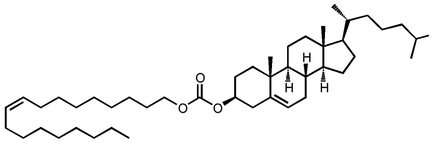	8.9
Tetrabutylammonium perchlorate (supporting electrolyte salt)	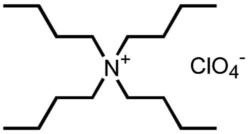	0.9
EBE (monomer)	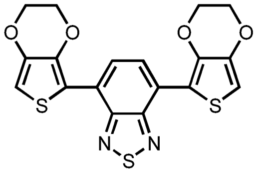	0.9

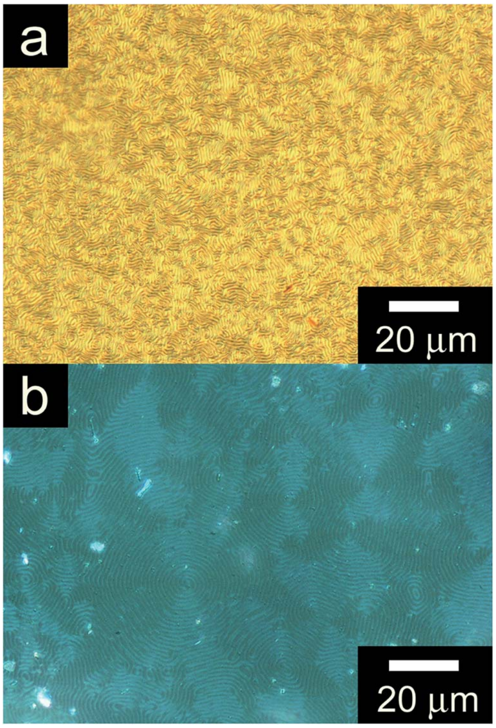

Fig. 2 POM images of the (a) fingerprint texture of the reaction mixture at room temperature and (b) transcribed fingerprint texture of polyEBE$_{CLC}$ at room temperature.

polymerisation. During the process, 6CB and COC can be removed during polymerisation by a phase-separation process. This mechanism can be the same as the results reported by Kihara *et al.*[47] Besides, washing with water and organic solvents flushes remaining 6CB, COC, TBAP and unreacted monomers from deposited polymers. The polymer thus obtained forms an intermolecular twisted structure (helical structure, Fig. 3d), which is similar to that of CLC. Such a process would be expected to produce a fingerprint structure in the polymer.[37] This polymer thus prepared in CLC is abbreviated as polyEBE$_{CLC}$.

Fourier transform infrared (FT-IR) absorption spectra of polyEBE$_{CLC}$, EBE (monomer), 6CB liquid crystal (matrix), and COC (a chiral inducer) are shown in Fig. 4. The CN triple bond vibration of the matrix LC appears at 2200 cm^{-1} for 6CB and C=O vibration at 1700 cm^{-1} for COC. PolyEBE$_{CLC}$ has no peaks at around 2200 cm^{-1} and 1700 cm^{-1} in the spectrum. The absence of these signals for polyEBE$_{CLC}$ in the FT-IR spectra indicates that neither 6CB nor COC remain in the polyEBE$_{CLC}$ film. This result confirms that the fingerprint texture of the polymer is derived from a pure polyEBE$_{CLC}$ film.

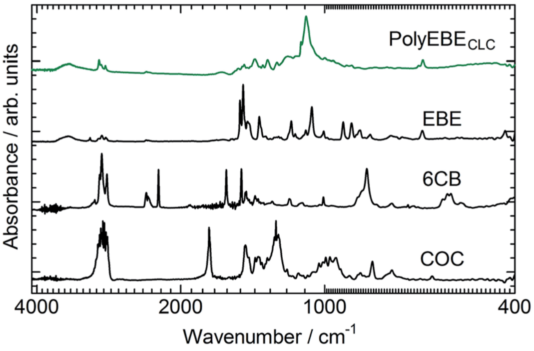

Fig. 4 FT-IR absorption spectra of polyEBE$_{CLC}$, EBE, 6CB and COC.

Electrochemical properties of polyEBE$_{CLC}$ were examined by cyclic voltammetry (Fig. 5). As a reference, we additionally prepared a polyEBE film by normal electrochemical polymerisation in acetonitrile solution. This polymer is abbreviated as polyEBE$_{ACN}$. Electrochemical measurements for the resultant polymer were carried out at scan rates of 10 to 100 mV s^{-1}, respectively, in acetonitrile containing 0.1 M TBAP. The potentials are estimated relative to a silver–silver ion (Ag/Ag$^+$) reference electrode. Cyclic voltammograms of polyEBE$_{CLC}$ and polyEBE$_{ACN}$ show oxidation and reduction signals at the same position. The polyEBE$_{CLC}$ film shows the same electrochemical response as polyEBE$_{ACN}$. This reflects that the redox properties depend on the primary structure of the polymers.

UV-vis absorption changes of polyEBE$_{CLC}$ with electrochemical oxidation and reduction were observed (Fig. 6). In the reduced state, two absorption maxima appeared near 725 nm and 425 nm (Fig. 6a). The 425 nm band is assignable to the π–π* transition. The 725 nm band is due to an intramolecular charge transfer (ICT) band typically observed from donor–acceptor structures. The band-edge bandgap of the polymer is estimated by the onset of the optical absorption to be 1.24 eV. This absorption band is changed drastically by the

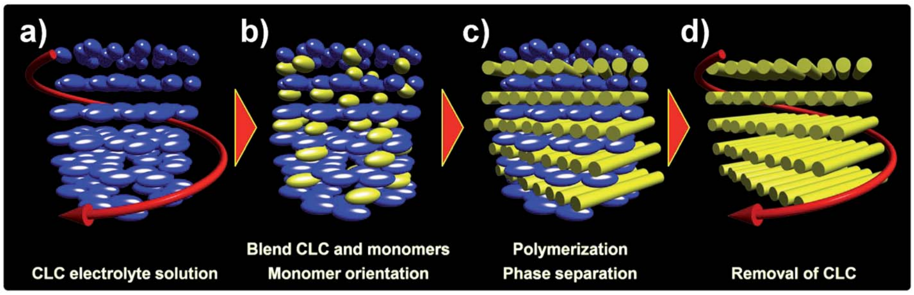

Fig. 3 Illustration of the mechanism of helical structure formation during electrochemical polymerisation in a CLC medium. Ellipsoids are CLC molecules (blue) and monomers (yellow); sticks are polymers.

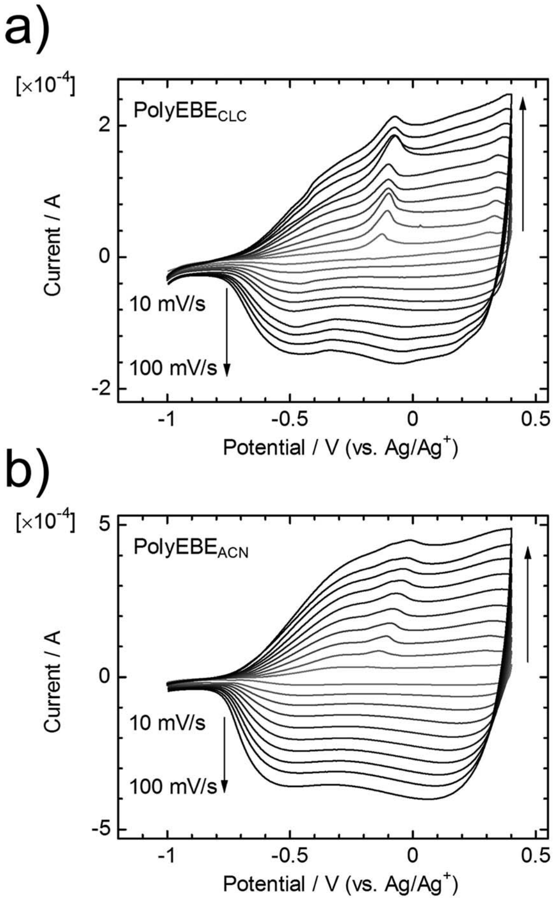

Fig. 5 Cyclic voltammograms of polyEBE observed by electrochemical polymerisation. (a) A polymer prepared in a cholesteric liquid crystalline medium and (2) a polymer prepared in acetonitrile electrolytic solution.

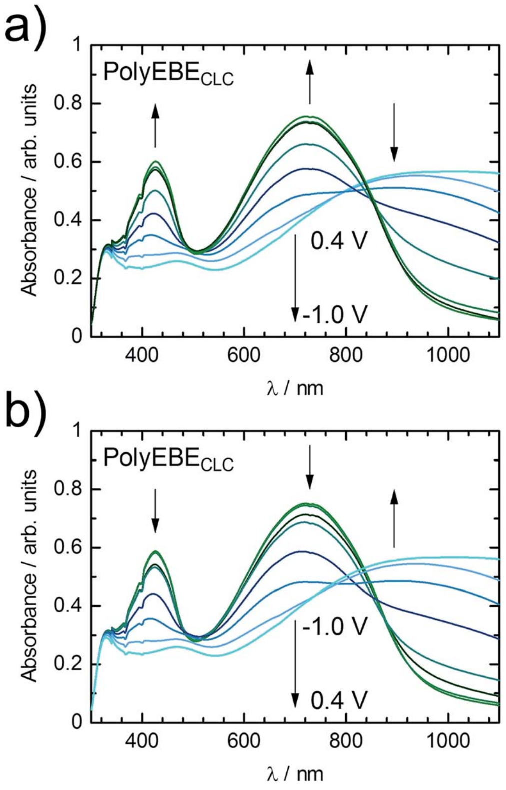

Fig. 6 Changes of UV-vis absorption spectra of a polyEBE$_{CLC}$ film in electrochemical reduction and oxidation (*vs.* Ag/Ag$^+$).

electrochemical redox process. In the oxidised state (Fig. 6b), the two bands decrease in intensity and a polaron band (doping band) appears at long wavelengths. This change is repeatable under electrochemical redox. Electrochromism of polyEBE films was observed during the electrochemical process. The change in colour is visually confirmed, as shown in Fig. 7b and d. The film exhibited green colour in the reduced state and blue colour in the oxidised state. This colour change is repeatable by electrochemical redox switching. The mesoscopic fingerprint structure of the film is maintained over several electrochemical redox processes (Fig. 7a and c). The same UV-vis observation was demonstrated for polyEBE$_{ACN}$ for comparison. As shown in Fig. 8, UV-vis absorption behaviour of polyEBE$_{ACN}$ by an electrochemical redox process is identical to polyEBE$_{CLC}$.

Circular dichroism (CD) of polyEBE$_{CLC}$ is also tunable by an electrochemical redox process, as shown in Fig. 9. CD spectra of polyEBE$_{CLC}$ have several peaks overlapping each other near absorption maxima. As a result, the observation showed two negative bisignate Cotton effects. These Cotton effects appear at around 720 nm and 440 nm, respectively. These values are in excellent agreement with the two peaks of UV-vis spectra (725 nm, 425 nm). Therefore, these Cotton effects can be attributed to ICT and π–π* transitions, respectively. Both the Cotton effects are strengthened from the oxidised state to the reduced state. This CD observation results indicate that polyEBE has structural chirality derived from its aggregated helical structure transcribed by CLC.

These changes of the CD spectra suggest that structural changes in the aggregated form of the helical structure may occur due to the electrochemical redox process, because the optical activity of the polymer derives from the structural chirality in a manner similar to CLC. Moreover, repeated changes in ellipticity at 860 nm and 410 nm in electrochemical oxidation and reduction were obtained as shown in Fig. 10. Applied voltages were cyclically swept 10 times from −1.0 V to 0.4 V at 50 mV s^{-1} with automatic control by the instrument. The ellipticities were retained completely after 10 cycles. This suggests that the polyEBE film is mechanically stable and can maintain its optical properties against an applied voltage within −1.0 V to 0.4 V.

A broad UV-vis absorption band in a longer wavelength region (800 nm) appearing in the oxidised state indicates the generation of polarons. In this state, a pair of a radical and a cation is generated along π-conjugated polymer chains. This behaviour can be detected by using electron spin resonance (ESR) spectroscopy. Fig. 11 shows changes in the ESR signals derived from radicals on polyEBE in the electrochemical redox processes. Both in reduction and oxidation processes, the signal displays the maximum value. In the oxidation process, further

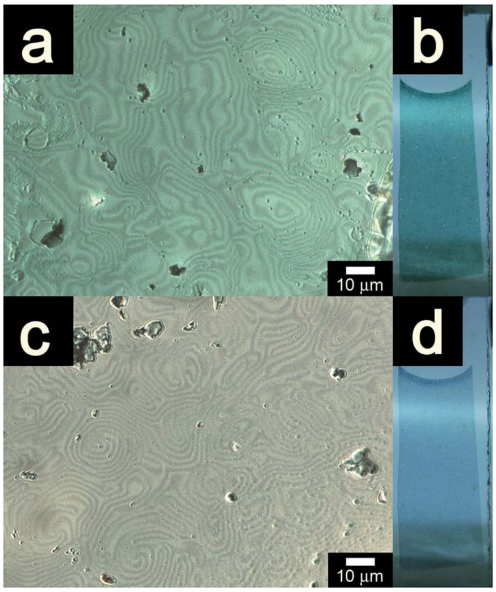

Fig. 7 POM and visual observation of electrochromism of polyEBE$_{CLC}$ in green (a and b) and blue (c and d) colours.

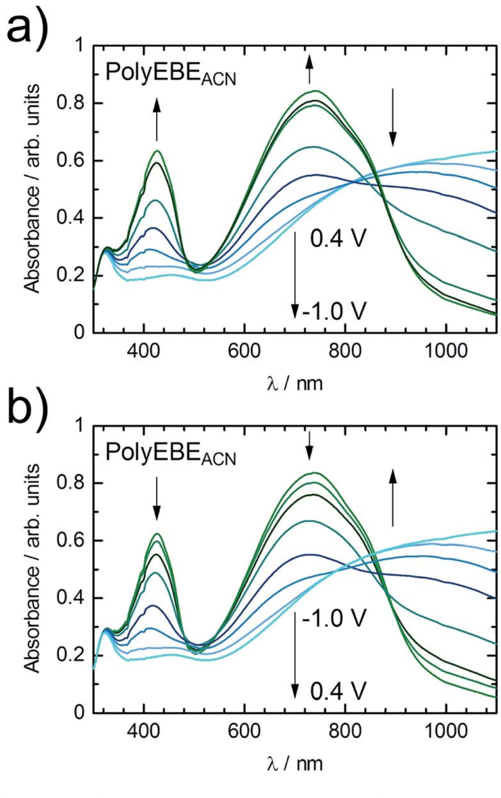

Fig. 8 Changes of UV-vis absorption spectra of a polyEBE$_{ACN}$ film in electrochemical reduction and oxidation (*vs.* Ag/Ag$^+$).

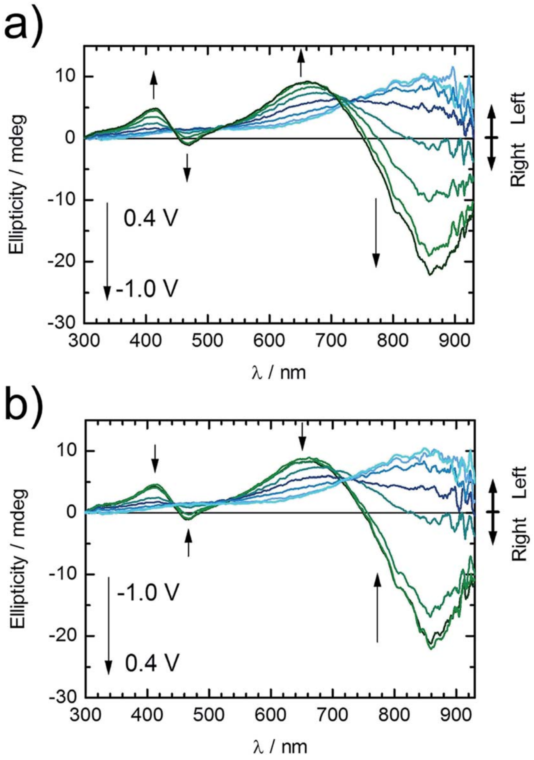

Fig. 9 CD spectra of polyEBE$_{CLC}$ with applied voltage (*vs.* Ag/Ag$^+$).

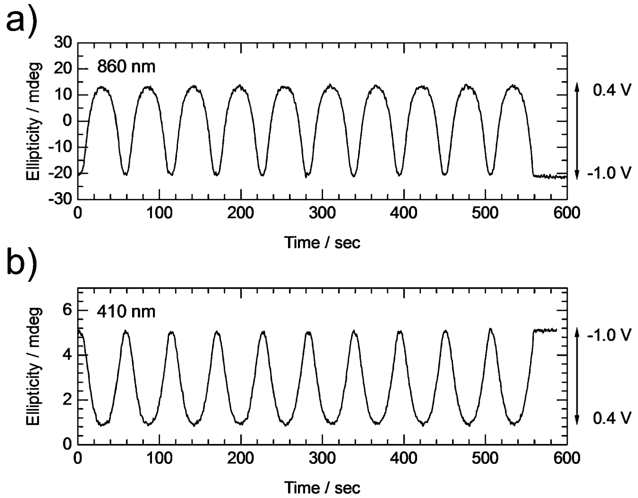

Fig. 10 Repeating changes in the ellipticity of polyEBE$_{CLC}$ at 860 nm (a) and 410 nm (b) in electrochemical oxidation and reduction. Applied voltage was cyclically swept 10 times from −1.0 V to 0.4 V at 50 mV s^{-1} (*vs.* Ag/Ag$^+$).

electron extraction from the polaron state results in the generation of bipolarons. In this state, the main charge carrier is a pair of two cations (dications) in place of radical cations. Thus, the ESR intensity is decreased from the maximum in the oxidation process due to the change of species of the carrier from radical cations to dications. After the oxidation, the ESR signal was repeatedly changed in the redox process. This repeated change can be performed in further cyclic sweeps, as well as change in the UV-vis and the CD.

Focusing on differences between electrochemical reduction and oxidation of polyEBE$_{CLC}$, changes in the *g*-value and peak height of ESR spectra were examined. These changes are summarised in Fig. 12, exhibiting hysteresis behaviour. This hysteresis may be due to the difference in the diffusion rate

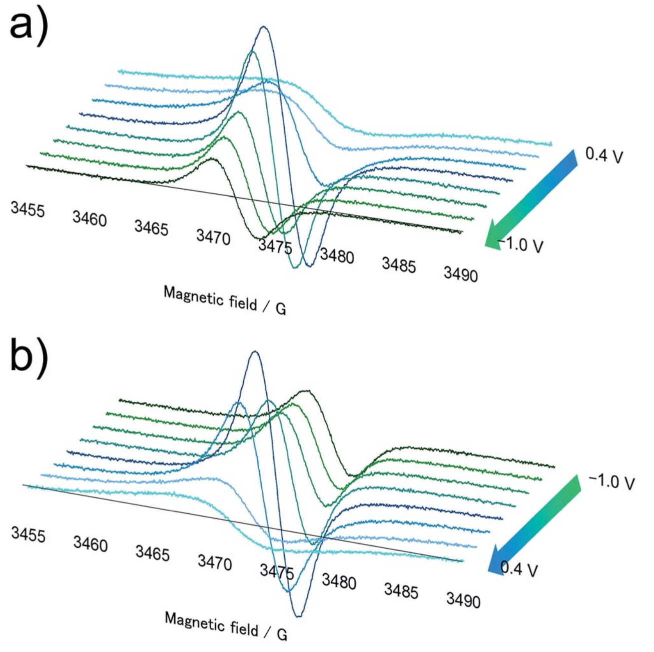

Fig. 11 Changes of ESR spectra of the polyEBE$_{CLC}$ film in electrochemical reduction (a) and oxidation (b) (*vs.* Ag/Ag$^+$).

between intrusion and extrusion (doping–dedoping or oxidation–reduction) of ions. The same behaviour can be observed in the UV-vis absorption and the CD. Compared to those of polyEBE$_{ACN}$, responsiveness to the change in applied voltage is fast. This means that hysteresis in the applied voltage of polyEBE$_{CLC}$ is smaller than that of polyEBE$_{ACN}$. Differences in the crystallinity of these polymer films might affect the diffusion of the ions.

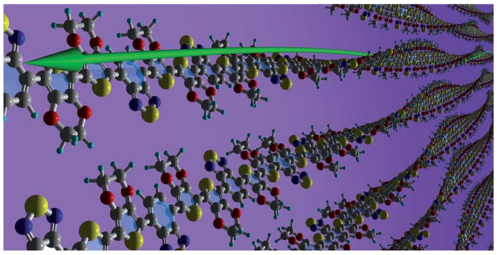

Fig. 13 A graphic image of "chiralion," a radical cation moving along the polyEBE$_{CLC}$ chain with a helical aggregation structure.

PolyEBE films prepared by electrochemical polymerisation using CLC medium have an ordered structure consisting of polymer chains, which is transcribed from the CLC medium. The fingerprint structure should be twisting along with the CLC order. Charge carriers such as radical cations (polarons) and dications (bipolarons) can move along the helical chains. Such charge carriers delocalised along the chiral conjugated system, referred to as "chiralions," are observed (Fig. 13).

4 Conclusions

A donor–acceptor type chiral polymer film showing a fingerprint surface structure was prepared successfully by electrochemical polymerisation in a cholesteric liquid crystalline medium. This polymer film appears green in the reduced state and blue in the oxidised state. Colour changes and CD signals of the film are repeatable after electrochemical oxidation and reduction. The generation of charge carriers in polaron and bipolaron states was confirmed by using the ESR. Chiralions, charge carriers delocalised along the optically active π-conjugated system, are

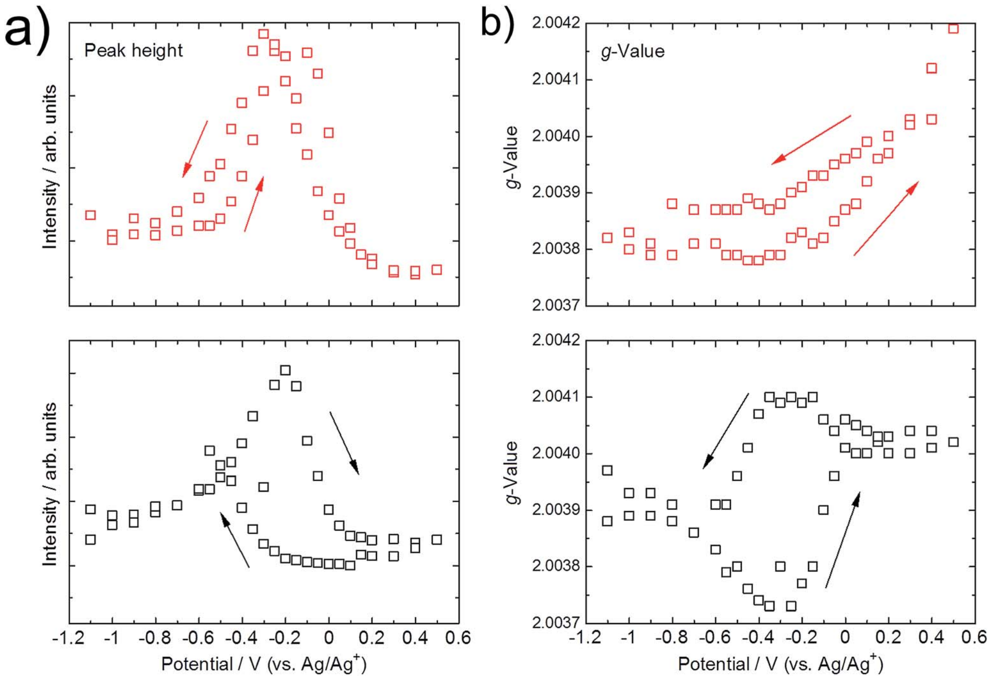

Fig. 12 ESR changes of peak height (a) and *g*-value (b) of polyEBE$_{CLC}$ (above) and polyEBE$_{ACN}$ (below) in electrochemical reduction and oxidation.

proposed. This polyEBE$_{CLC}$ may be the first example of an ICT-type conjugated polymer with electro-optical activity.

Acknowledgements

We would like to thank the Chemical Analysis Division Research Facility Centre for Science and Technology, and Glass Work Shop, of the University of Tsukuba.

References

1 K. Wagner, R. Byrne, M. Zanoni, S. Gambhir, L. Dennany, R. Breukers, M. Higgins, P. Wagner, D. Diamond, G. G. Wallace and D. L. Officer, *J. Am. Chem. Soc.*, 2011, **133**, 5453–5462.

2 F. B. Koyuncu, E. Sefer, S. Koyuncu and E. Ozdemir, *Macromolecules*, 2011, **44**, 8407–8414.

3 E. Collini and G. D. Scholes, *Science*, 2009, **323**, 369–373.

4 C. M. Cardona, W. Li, A. E. Kaifer, D. Stockdale and G. C. Bazan, *Adv. Mater.*, 2011, **23**, 2367–2371.

5 S. Song, S. Park, S. Kwon, B. H. Lee, J. A. Kim, S. H. Park, Y. Jin, J. Lee, I. Kim, K. Lee and H. Suh, *Synth. Met.*, 2012, **162**, 1936–1943.

6 E. Nasybulin, S. Wei, M. Cox, I. Kymissis and K. Levon, *J. Phys. Chem. C*, 2011, **115**, 4307–4314.

7 M. H. Han, H. J. Song, T. H. Lee, J. Y. Lee, D. K. Moon and J. R. Haw, *Synth. Met.*, 2012, **162**, 2294–2301.

8 S. Ko, E. T. Hoke, L. Pandey, S. Hong, R. Mondal, C. Risko, Y. Yi, R. Noriega, M. D. McGehee, J.-L. Brédas, A. Salleo and Z. Bao, *J. Am. Chem. Soc.*, 2012, **134**, 5222–5232.

9 S. I. Cho, W. J. Kwon, S.-J. Choi, P. Kim, S.-A. Park, J. Kim, S. J. Son, R. Xiao, S.-H. Kim and S. B. Lee, *Adv. Mater.*, 2005, **17**, 171–175.

10 Y. Pang, X. Li, H. Ding, G. Shi and L. Jin, *Electrochim. Acta*, 2007, **52**, 6172–6177.

11 P. Taranekar, T. Fulghum, A. Baba, D. Patton and R. Advincula, *Langmuir*, 2007, **23**, 908–917.

12 S. S. Pinnock, C. N. Malele, J. Che and W. E. Jones Jr, *J. Fluoresc.*, 2012, **22**, 583–589.

13 B.-G. Kim, E. J. Jeong, H. J. Park, D. Bilby, L. J. Guo and J. Kim, *ACS Appl. Mater. Interfaces*, 2011, **3**, 674–680.

14 T. J. White, M. E. McConney and T. J. Bunning, *J. Mater. Chem.*, 2010, **20**, 9832–9847.

15 K. Rameshbabu, A. Urbas and Q. Li, *J. Phys. Chem. B*, 2011, **115**, 3409–3415.

16 S. N. Lee, L.-C. Chien and S. Sprunt, *Appl. Phys. Lett.*, 1998, **72**, 885–887.

17 G. Solladié and R. G. Zimmermann, *Angew. Chem., Int. Ed. Engl.*, 1984, **23**, 348–362.

18 T. J. White, R. L. Bricker, L. V. Natarajan, N. V. Tabiryan, L. Green, Q. Li and T. J. Bunning, *Adv. Funct. Mater.*, 2009, **19**, 3484–3488.

19 V. Sharma, M. Crne, J. O. Park and M. Srinivasarao, *Science*, 2009, **32**, 449–451.

20 D. G. Stavenga, B. D. Wilts, H. L. Leertouwer and T. Hariyama, *Philos. Trans. R. Soc., B*, 2011, **366**, 709–723.

21 S. Lowrey, L. D. Silva, I. Hodgkinson and J. Leader, *J. Opt. Soc. Am. A*, 2007, **24**, 2418–2425.

22 G. A. Sotzing and J. R. Reynolds, *Chem. Mater.*, 1996, **8**, 882–889.

23 S. Akoudad and J. Roncali, *Synth. Met.*, 1999, **101**, 149.

24 P. Si, Q. Chi, Z. Li, J. Ulstrup, P. J. Møller and J. Mortensen, *J. Am. Chem. Soc.*, 2007, **129**, 3888–3896.

25 H. Yamamoto, M. Oshima, M. Fukuda, I. Isa and K. Yoshino, *J. Power Sources*, 1996, **60**, 173–177.

26 J. Zhang, L.-B. Kong, B. Wang, Y.-C. Luo and L. Kang, *Synth. Met.*, 2009, **159**, 260–266.

27 R. J. Mortimer, A. L. Dyer and J. R. Reynolds, *Displays*, 2006, **27**, 2–18.

28 M. C. Turhan, M. Weiser, H. Jha and S. Virtanen, *Electrochim. Acta*, 2011, **56**, 5347–5354.

29 M. S. Cho, Y. Y. Yun, J. D. Nam, Y. Son and Y. Lee, *Synth. Met.*, 2008, **158**, 1043–1046.

30 T. Hatano, A.-H. Bae, M. Takeuchi, N. Fujita, K. Kaneko, H. Ihara, M. Takafuji and S. Shinkai, *Angew. Chem.*, 2004, **116**, 471–475.

31 Y. H. Wijsboom, A. Patra, S. S. Zade, Y. Sheynin, M. Li, L. J. W. Shimon and M. Bendikov, *Angew. Chem., Int. Ed.*, 2009, **48**, 5443–5447.

32 H. Goto, *J. Mater. Chem.*, 2009, **19**, 4914–4921.

33 H. Yoneyama, A. Tsujimoto and H. Goto, *Macromolecules*, 2007, **40**, 5279–5283.

34 K. Kawabata, H. Yoneyama and H. Goto, *Mol. Cryst. Liq. Cryst.*, 2009, **515**, 3–15.

35 K. Kawabata, H. Yoneyama and H. Goto, *Polym. Chem.*, 2010, **1**, 1606–1608.

36 G. J. McEntee, P. J. Skabara, F. Vilela, S. Tierney, I. D. W. Samuel, S. Gambino, S. J. Coles, M. B. Hursthouse, R. W. Harrington and W. Clegg, *Chem. Mater.*, 2010, **22**, 3000–3008.

37 K. Kawabata and H. Goto, *Chem. Lett.*, 2009, **38**, 706–707.

38 A. Durmus, G. E. Gunbas, P. Camurlu and L. Toppare, *Chem. Commun.*, 2007, 3246–3248.

39 S. Tarkuc, E. K. Unver, Y. A. Udum and L. Toppare, *Eur. Polym. J.*, 2010, **46**, 2199–2205.

40 I. Schwendeman, R. Hickman, G. Sönmez, P. Schottland, K. Zong, D. M. Welsh and J. R. Reynolds, *Chem. Mater.*, 2002, **14**, 3118–3122.

41 G. Sönmez, C. K. F. Shen, Y. Rubin and F. Wudl, *Angew. Chem., Int. Ed.*, 2004, **43**, 1498–1502.

42 G. Sönmez, H. B. Sönmez, C. K. F. Shen, R. W. Jost, Y. Rubin and F. Wudl, *Macromolecules*, 2005, **38**, 669–675.

43 G. E. Gunbas, A. Durmus and L. Toppare, *Adv. Mater.*, 2008, **20**, 691–695.

44 W.-H. Chen, K.-L. Wang, D.-L. Liaw, K.-R. Lee and J.-Y. Lai, *Macromolecules*, 2010, **43**, 2236–2243.

45 S. S. Zhu and T. M. Swager, *J. Am. Chem. Soc.*, 1997, **119**, 12568–12577.

46 G. Gottarelli, M. Hibert, B. Samori, G. Solladié, G. P. Spada and R. Zimmermann, *J. Am. Chem. Soc.*, 1983, **105**, 7318–7321.

47 H. Kihara and T. Miura, *Polymer*, 2005, **46**, 10378–10382.